

REPORT DOCUMENTATION PAGE

Form Approved
OMB No. 0704-0188

Public reporting burden for this collection of information is estimated to average 1 hour per response, including the time for reviewing instructions, searching existing data sources, gathering and maintaining the data needed, and completing and reviewing this collection of information. Send comments regarding this burden estimate or any other aspect of this collection of information, including suggestions for reducing this burden to Department of Defense, Washington Headquarters Services, Directorate for Information Operations and Reports (0704-0188), 1215 Jefferson Davis Highway, Suite 1204, Arlington, VA 22202-4302. Respondents should be aware that notwithstanding any other provision of law, no person shall be subject to any penalty for failing to comply with a collection of information if it does not display a currently valid OMB control number. PLEASE DO NOT RETURN YOUR FORM TO THE ABOVE ADDRESS.

DTIC COPY

1. REPORT DATE (DD-MM-YYYY) 10-11-2009		REPRINT			
4. TITLE AND SUBTITLE A new spectro-polarimeter for solar prominence and filament magnetic field measurements			5a. CONTRACT NUMBER		
			5b. GRANT NUMBER		
			5c. PROGRAM ELEMENT NUMBER 61102F		
6. AUTHOR(S) D.F. Elmore, R. Casini, G.L. Card, M. Davis, A. Lecinski, R. Lull, P.G. Nelson, and S. Tomczyk			5d. PROJECT NUMBER 2301		
			5e. TASK NUMBER RD		
			5f. WORK UNIT NUMBER Z1		
7. PERFORMING ORGANIZATION NAME(S) AND ADDRESS(ES) High Altitude Observatory National Center for Atmospheric Research P.O. Box 3000 Boulder, CO 80307-3000			8. PERFORMING ORGANIZATION REPORT NUMBER		
9. SPONSORING / MONITORING AGENCY NAME(S) AND ADDRESS(ES) AF Research Laboratory/RVBXS* 29 Randolph Road Hanscom AFB MA 01731-3010			10. SPONSOR/MONITOR'S ACRONYM(S) AFRL/RVBXS		
			11. SPONSOR/MONITOR'S REPORT NUMBER(S) AFRL-RV-HA-TR-2009-1103		
12. DISTRIBUTION / AVAILABILITY STATEMENT Approved for Public Release; Distribution Unlimited. Also AFRL/RVBXS, Sunspot, NM.					
13. SUPPLEMENTARY NOTES REPRINTED FROM: "Ground-based and Airborne Instrumentation for Astronomy II", edited by McLean, I.S. and Casali, M.M., Proceedings of the SPIE, Vol 7014, pp 701416-701416-10, 2008					
14. ABSTRACT We are constructing a spectro-polarimeter using the 40-cm coronagraph at the Evans Solar Facility of the National Solar Observatory in Sunspot, NM for the purpose of measuring the vector magnetic field in prominences and filaments. The Prominence Magnetometer (ProMag) is comprised of a polarization modulation package and a spectrograph. The modulation optics are located at the prime focus of the coronagraph along with calibration optics and a beamsplitter that creates two beams of orthogonal Stokes states. The spectrograph resides at the coude focus of the coronagraph. The polarizations of the two chromospheric lines of neutral helium, at 587.6 nm and 1083.0 nm, are to be observed simultaneously. We present details of the design of the spectro-polarimeter.					
15. SUBJECT TERMS Spectro-Polarimetry Sun Magnetic Fields					
16. SECURITY CLASSIFICATION OF:			17. LIMITATION OF ABSTRACT	18. NUMBER OF PAGES	19a. NAME OF RESPONSIBLE PERSON
a. REPORT UNCLAS	UNCLAS	c. THIS PAGE UNCLAS	SAR		R. Altrock
					19b. TELEPHONE NUMBER (include area code) 575-434-7016

A new spectro-polarimeter for solar prominence and filament magnetic field measurements

David F. Elmore, Roberto Casini, Greg L. Card, Marc Davis, Alice Lecinski, Ron Lull, Peter G. Nelson, Steven Tomczyk

High Altitude Observatory, National Center for Atmospheric Research,*
P.O. Box 3000, Boulder, CO 80307-3000, U.S.A.

DTIC COPY

ABSTRACT

We are constructing a spectro-polarimeter using the 40-cm coronagraph at the Evans Solar Facility of the National Solar Observatory in Sunspot, NM for the purpose of measuring the vector magnetic field in prominences and filaments. The Prominence Magnetometer (ProMag) is comprised of a polarization modulation package and a spectrograph. The modulation optics are located at the prime focus of the coronagraph along with calibration optics and a beamsplitter that creates two beams of orthogonal Stokes states. The spectrograph resides at the coude focus of the coronagraph. The polarizations of the two chromospheric lines of neutral helium, at 587.6 nm and 1083.0 nm, are to be observed simultaneously. We present details of the design of the spectro-polarimeter.

Keywords: Spectro-Polarimetry, Sun, Magnetic Fields

1. INTRODUCTION

The importance of measuring magnetic fields in the prominences and filaments embedded in the hot solar corona has long been recognized in solar physics research. Pioneering observations were carried out in the 1970s and 1980s.^{1,2} For almost two decades little further work was done until the past few years, when the major difficulties in instrumentation and spectro-polarimetric interpretation could be addressed. The new instrumental capabilities now offer the prospect of observing prominence magnetic fields on a regular basis, opening up a unique opportunity in prominence research.

Recent attempts at measuring magnetic fields in prominences and filaments have been carried out at the Dunn Solar Telescope of the National Solar Observatory in Sacramento Peak (NSO/SP, Sunspot, NM), and at the French-Italian solar telescope THÉMIS (Tenerife, Canary Islands, Spain). While these instruments are adequate for doing high precision spectro-polarimetry on the disk and on the brightest structures off the limb, the high level of instrumental scattered light is a strong impediment for the investigation of fainter and higher prominences. In addition, both telescopes are intensively used by the solar community for many different research programs, so they cannot be made available to run a monitoring program of prominence/filament observations.

For these reasons we decided to build a new spectro-polarimeter, optimized for the observation of the chromospheric lines of He I at 587.6 nm (D_3) and at 1083 nm, and to install it at the coronagraph of the Evans Solar Facility (ESF) of the NSO/SP. This telescope offers a very low level of instrumental scattered light, and for the past two decades has been used primarily for a coronal photometry program, which presently occupies only a small fraction of the day, three times a week. With this new instrument, we plan to initiate a regular observing program of prominences and filaments (as well as of other interesting chromospheric regions) with the goal of understanding the many topologies of the magnetic field in these structures, and how they connect with the global magnetic field in the solar corona.

*The National Center for Atmospheric Research is sponsored by the National Science Foundation.

Further author information: (Send correspondence to R.C.)

R.C.: E-mail: casini@ucar.edu, Telephone: 1 303 497 1508

20091207050

2. OBSERVATIONAL REQUIREMENTS

The study of chromospheric structures, like prominences and filaments, must take into account the particular conditions of illumination by the underlying photosphere, and how the state of atomic excitation in the plasma is determined by such conditions. The geometric height of the observed point, and the angular distribution of the emergent radiation from the photosphere (*center-to-limb variation*; CLV), determine a condition of anisotropic illumination of the observed point. This induces anisotropies in the population of the atomic levels, as well as atomic coherence within the levels. These peculiar properties of the excited state of the atoms are encoded in the polarization of the scattered radiation, which is traditionally measured in terms of the four Stokes parameters, I, Q, U, V , and are sensitive to the presence of magnetic fields through the Hanle and Zeeman effects, and the effect of level-crossing interferences.³ Therefore, a careful modeling of scattering polarization in spectral lines observed in the chromosphere can reveal the magnetic structure of the observed regions.

There are several reasons for adopting the two chromospheric He I lines for prominence and filament diagnostics. The He I D₃ line has a magnetic range of sensitivity to the Hanle effect that overlaps the weak fields that are expected in quiescent prominences and filaments ($B \lesssim 100$ G). Its diagnostic potential has been clearly demonstrated in pioneering work on prominence magnetometry,^{1,2,4-6} and confirmed by more recent studies.⁷⁻¹⁰ Spectro-polarimetry in the He I 1083 nm multiplet has become practical only during the last decade, thanks to the development of fast IR detector arrays. This line complements the diagnostic content of He I D₃, since it forms in a "saturated" regime of the Hanle effect (i.e., of fully relaxed atomic coherences) from weak fields of at least 5-10 G up to strong fields around 10³ G, when finally level-crossing interferences start to appear. Because level crossing sets in so late in the upper level of He I 1083 nm, unlike the case of He I D₃, the amount of net circular polarization (NCP) in this line is always expected to be very small. In particular, this provides a useful tool for the control of S -to- V crosstalk (with $S = I, Q, U$) in the instrument. Finally, because the two chromospheric He I lines belong to the same atomic model, the forward modeling part of data inversion is greatly facilitated by adopting these lines.

The optimization of modulation efficiency of the polarimeter at the wavelengths of the two chromospheric He I lines is therefore of primary importance. As it turns out, the polarimeter is fairly achromatic, with good levels of modulation efficiency anywhere between 570 nm and 1200 nm. This fact allows the investigation of other important chromospheric lines, like the Na I D doublet (589.3 nm), H α (656.3 nm), and the Ca II IR triplet (849.8 nm, 854.2 nm, 866.2 nm), as well as the forbidden coronal lines of Fe XIII (1074.7 nm and 1079.8 nm). In particular, H α adds the possibility of plasma density diagnostics through the modeling of the NCP induced by the micro-turbulent electric plasma fields.¹¹

For a correct magnetic diagnostic one needs sufficient spectral information on the four polarization Stokes parameters, I, Q, U, V , in order to constrain the inversion of the data by profile fitting. He I D₃ poses the stricter constraint, since the two visible components of the multiplet are less than 0.04 nm apart. For comparison, the two visible components of the He I 1083 nm multiplet are about three times more separated. He I D₃ being a secondary line, it is optically thin in most cases. For this reason its contrast on the solar disk is very small, and it is best observed in emission in solar prominences. The brightness of these structures varies approximately from less than 0.1% up to 1% of the solar disk intensity. On the contrary, the resonant transition at He I 1083 nm is relatively easily observed both in emission off the limb and in absorption on the disk.

Recent observations of prominences from space with Hinode, at 0.3 arcsec spatial resolution, show very clearly the small-scale, filamentary structure of these objects. On the other hand, theoretical models of prominences and filaments prescribe that the magnetic topology should be coherent at a spatial scale significantly larger than that. This argument seems to be confirmed by recent observations of a quiescent prominence.⁹ It was found that the adopted model of scattering polarization, assuming a single magnetic component within the spatial resolution element, started breaking down if the data were binned beyond approximately 3-arcsec pixels. This case seems to suggest that a spatial resolution of 2 to 3 arcsec should be adequate for a monitoring program of prominence magnetometry.

2.1 Instrument Requirements

Observational requirements lead to requirements on the instrument, Table 1. In order to achieve polarimetry to a level of 10^{-3} , a dual beam polarimeter design is needed to reduce seeing induced cross talk.¹²

Table 1. Instrument requirements derived from observational requirements

Spectral lines:	587.6 nm and 1083.0 nm, simultaneously and co-spatially 656.3 nm and 1083.0 nm, simultaneously and co-spatially Other lines one at a time between 587.6 nm and 1350 nm (goal)
Field:	Span a prominence > 100 arcsec
Spatial resolution:	2 to 3 arcsec
Spectral resolution:	5 pm @ 587.6 nm
Polarimetry:	I, Q, U, V : noise < $10^{-3} I_c$ (goal: < $5 \times 10^{-4} I_c$), dual-beam

2.2 Constraints

Camera requirements are met by an existing PixelVision Pluto camera for visible wavelengths and by a relatively small format FLIR Alpha Near Infrared (NIR) camera. The ESF 40-cm coronagraph is of sufficiently large aperture to achieve the required signal to noise, additional instrumentation can be added to the facility, and its use leverages the long history of collaborative projects between HAO and NSO.

Table 2. Constraints on the ProMag design.

Cameras:	PixelVision Pluto, 652×488 , $12 \mu\text{m}$ pixels FLIR Alpha InGaAs 320×256 , $30 \mu\text{m}$ pixels
Telescope:	Evans Solar Facility, 40-cm coronagraph, East bench, and ESF control.

3. INSTRUMENT DESCRIPTION

3.1 Telescope

The 40-cm aperture coronagraph, Figure 1, in the ESF has low scatter, and low polarization preceding the prime focus. Placing the polarization modulator and analyzer at the prime focus reduces the influence of following optics on the polarization measurement. The polarimeter at the prime focus must rotate so that the orientation of the spatially separated dual beams is as desired (normally radial). An image rotator just in front of the spectrograph is then required to align these beams with the slit. The telescope has been modeled in ZEMAX, Table 3.

Table 3. 40-cm coronagraph specification.

Focal Length:	11916 mm
Plate Scale:	$57.77 \mu\text{m}/\text{arcsec}$, $17.31 \text{ arcsec}/\text{mm}$
Field of View:	$160 \text{ arcsec} \times 320 \text{ arcsec}$

The polarimeter design, Figure 2, calls for a pre-inverse occulter 25 mm in diameter as part of the heat shield ahead of all prime focus optical elements. Also in the heat shield is an inverse occulter of the proper diameter for the coronal photometry program. In the ProMag path, there is an inverse occulter mid way between the focal points for 587.6 nm and 1083.0 nm. The size of this aperture is $10 \text{ mm} \times 17 \text{ mm}$ allowing an unvignetted $160 \text{ arcsec} \times 320 \text{ arcsec}$ field of view. Two sides of this inverse occulter have curved surfaces to match the mean diameter of the Sun. The radius of curvature of the mean solar image is 37.50 mm.

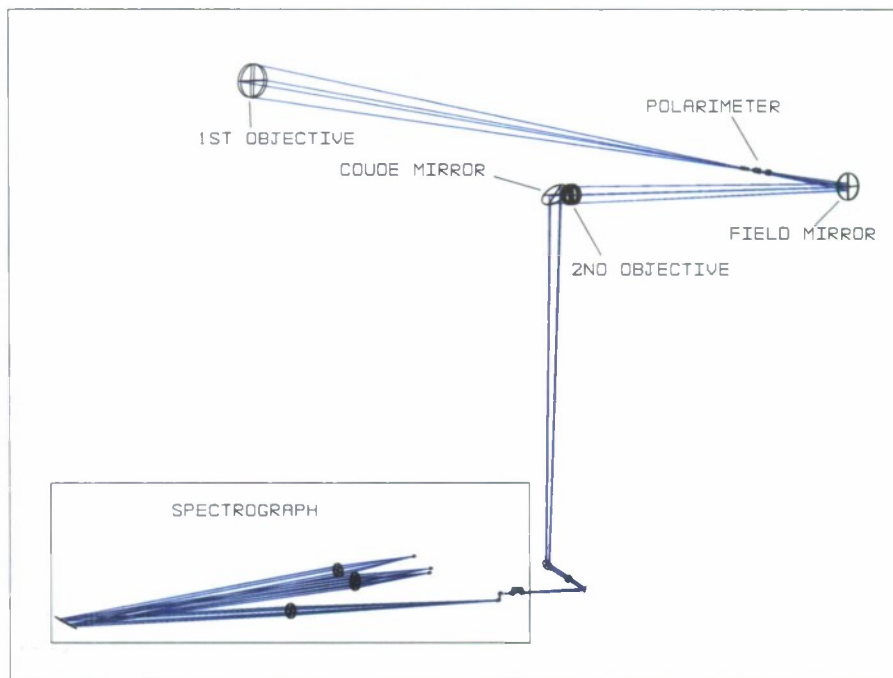


Figure 1. Optical configuration of ProMag. All optics through the coude mirror are in the dome of the ESF. Remaining optics reside in the observing room and include a new spectrograph optimized for ProMag.

A seven element second objective designed by Richard B. Dunn, does a good job of eliminating chromatic aberration over visible wavelengths. Between 587.6 nm and 1083.0 nm, however, there is a focal shift. For the coronagraph alone without the ProMag optics this shift is 25 mm with the 1083.0 nm image ahead of the 587.6 nm image (opposite in sign to what happens with a singlet lens). The focal positions of the two lines are brought into closer alignment due to the considerable thickness of glass added by the image rotator. The result is focal positions within about 6 mm. Without correcting focus, the calculated geometric spot diameter at the slit is comparable to the slit size for both wavelengths.

3.2 Polarization modulation/analysis unit

Polarization modulation and analysis, Figure 2, are accomplished at prime focus to avoid instrumental polarization before the modulator and variation of polarization response with solar elevation caused by the coude mirror. It has two positions, one for prominence magnetometry, whereas the other has a choice of two inverse occulters that can be used for the coronal photometer program. The modulator consists of a stack of six ferroelectric liquid crystals (FeLC). In front of the modulator is a UV blocking filter to protect the liquid crystal material. A calibration linear polarizer and calibration retarder can simultaneously be placed in the beam in front of all other optics. The linear polarizer and retarder rotate independently to any angle. The calibration stage has a dark position clear and calibration positions. Behind the liquid crystals is a Wollaston prism, a half-wave retarder, and another Wollaston prism. The prisms separate the two orthogonally polarized beams by approximately 9 mm then make them parallel. The entire polarimeter rotates so that the beam separation from the Wollaston prisms can be placed in the solar radial direction (or 90° from it) for any given solar azimuth.

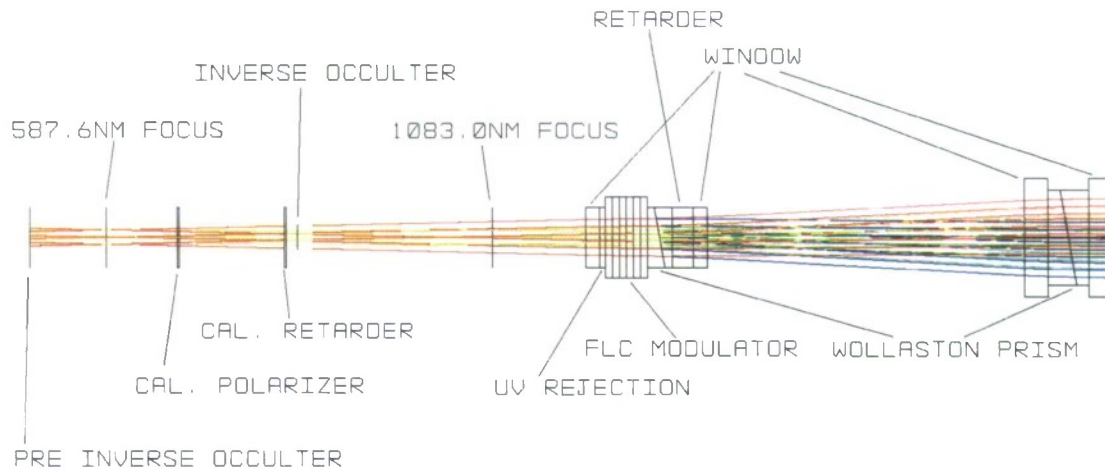


Figure 2. ProMag polarimeter at the coronagraph prime focus. The polarimeter is temperature controlled to 30° C and rotates about the optical axis.

3.3 Spectrograph

The Prominence Magnetometer spectrograph is constructed on the east bench of the observing room at the coude feed of the 40-cm coronagraph, Figure 3. It uses a 110 line/mm, 64° blaze angle grating from Newport RGL. A slit width of 72 μm is equivalent to 1.24 arcsec on the Sun. This is the nominal width providing spatial resolution between 2 and 3 arcseconds and is a multiple of the spatial pixel size. Since there is sufficient flux to avoid read noise, pixels are not binned in the camera though could be after the fact to improve signal to noise. Refractive optics are used, as opposed to off-axis mirrors, since they are easy to align, relatively inexpensive, and provide comfortable separation between the optics.

Table 4. Spectral sample sizes for 'visible' and infrared cameras.

FLIR Alpha spatial sample:	1.57 arcsec/pixel	
Pluto pixel sample:	0.63 arcsec/pixel	
Pluto spatial sample:	1.88 arcsec	(3 Pluto pixels)
Slit spatial sample sizes:	1.88 arcsec @ 108 μm	(3 Pluto pixels)
	1.57 arcsec @ 90 μm	(1 FLIR pixel)
	1.25 arc seconds @ 72 μm	(2 Pluto pixels)
	0.63 arc seconds @ 36 μm	(1 Pluto pixel)

The spectrograph uses a collimator lens with 3 m focal length and camera lenses of 1 m focal length. Angles of reflection are nearly the same for 587.6 and 656.3 (52°), and for 854.2 and 1083.0 (50°). Spectral sample sizes, Table 4, are compatible with the instrument requirements.

An angle of incidence of 67° is used so that the two primary lines fall comfortable away from the input beam. Both lines are detected with good efficiency and spectral resolution meeting the requirement. Calculations of spectral resolution, Table 5, assume a slit width of 72 μm, 1.24 arcsec. Resolution shown is the root sum square of the spectral slit width, spectral pixel width, and grating resolution. Some additional lines are shown. Due to angles of reflection for various lines, an arbitrary combination is not possible.

The full length of the Pluto camera CCD is needed to record the two spatially separated beams along the long, 652 pixel, axis of the detector. Of these, 255 are illuminated by each unvignetted beam and the two beams are separated by 94 pixels. The short 488 pixel axis is in the spectral direction. The FLIR Alpha camera has 320 spatial pixels and 256 spectral pixels. Spatially there are 102 pixels illuminated in each beam and 38 pixels separate the two beams.

Table 5. Spectral resolutions calculated from the spectrograph geometry, spectral slit width, spectral pixel width, and grating resolution.

Wavelength (nm)	Pixel sample (pm)	Slit sample (pm)	RSS Resolution (pm)	Length (nm)	Efficiency
587.6	1.78	3.05	3.64	0.87	0.66
1083.0	5.45	5.68	8.43	5.58	0.97
656.3	2.04	3.41	4.12	0.99	0.87
854.2	2.88	4.49	5.66	1.41	0.93
1435.0	8.60	7.75	12.80	8.81	0.37

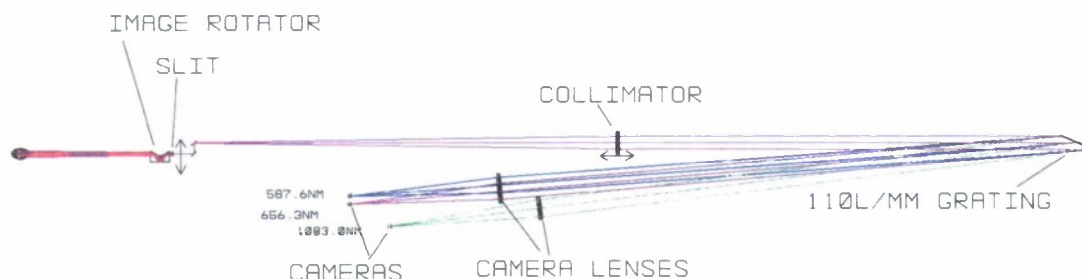


Figure 3. The spectrograph layout. The slit is translated in the direction of the arrows to scan a prominence. In order to maintain a collimated beam on the grating, the collimator translates along with the slit.

3.4 Flux Budget

A flux budget, Figure 4, has been constructed using estimates for transmissions of all the optical elements, nominal spatial sample size, and spectrograph spectral sample size and efficiency. Assumed prominence brightness is 1% for visible lines and 2% for IR lines. Polarization signal to noise vs. wavelength is shown for a 14.6s integration per slit position. Prominence maps are made up of typically 100 slit positions requiring approximately a half hour. The polarization noise level is well below 10^{-3} for all wavelengths, even for the 1% of disk brightness assumed for the visible lines.

3.5 Control System

The NSO ESF control system is used to set up the telescope for the prominence observations. Pointing, occulting assembly X-Y-Z motion, O_2 focus, telescope aperture, diffuser in or out, and the position of relay optics are adjusted manually through the ESF control system. No connection is required between the ESF control system and the magnetometer control system.

The experiment control system times and performs switching of the FeLCs and distributes read strobes and modulator status to the cameras and camera control computers. It connects via TCP/IP to an 8-axis mechanism controller (Newport XPS) to position ProMag mechanisms. Polarimeter and image rotator angles can be synchronously driven when aligning to solar features, or independently driven, when correcting for motion of the coude image. Angles of the calibration optics are set by experiment control as well as their translation into or out of the beam. The slit and collimator lenses can be driven independently or, when mapping a prominence, moved in synchrony. The experiment control application consists of a table driven experiment control process and a graphical user interface process.

Camera control software is based upon that used for Spectro-Polarimeter for Infrared and Optical Regions (SPINOR).¹³ This is the existing "Netspin" application with TCP/IP control. This configuration expects strobes to the camera, and the computer receives modulator position information via TCP/IP.

3.6 Polarimetry

A polarimeter with excellent efficiency over the wavelength range of 588 nm to 1083 nm is required by ProMag. Rapid polarization modulation is important to remove seeing induced crosstalk of intensity into the polarization

Polarization Sensitivity vs. Wavelength

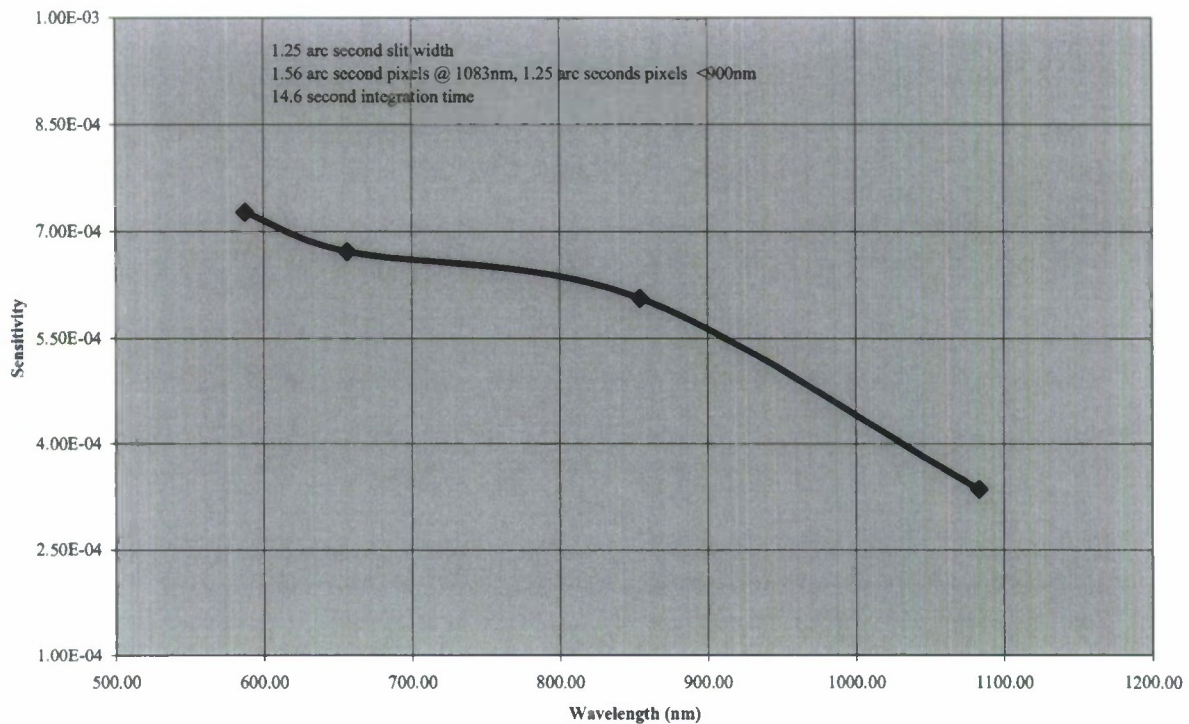


Figure 4. Estimated ProMag polarization sensitivity vs. wavelength. The model uses prominences 1% as bright as the solar disc for wavelengths less than 900 nm and 2% of the disc for 1083 nm.

parameters. Wide band fast modulators have been previously fabricated¹⁴ but not over a wavelength range this large. The ProMag polarization modulator is a pair of achromatic ferroelectric liquid crystal (FeLC) retarders. Each retarder is a Pancharatnam plate¹⁵ consisting of three FeLCs (Displaytech). Modeled polarization modulation efficiency of this design, Figure 5, is at least 0.5 between 587.6 nm and 1083.0 nm. Commonly FeLCs have a half-wave retardation and switch the orientation of the fast axis over a range of 45°, the cone angle. When placed between crossed polarizers, this creates an electrically switchable shutter. This application requires cone angles other than 45° and retardations other than 180°, products not available as catalog items. A number of FeLCs were characterized for retardation and cone angle using an imaging polarimeter. Retardation and cone angle were characterized as a function of LC material, temperature, drive voltage, LC thickness, and wavelength. An IDL application was constructed to model the performance of a polarimeter as a function of wavelength for a stack of six FeLCs grouped as two Pancharatnam plates. The final design optimizes each FeLC for material, thickness (using standard ball spacer sizes), clocking of the retardation axis, and drive voltage in the range of 3 V to 7 V. A control temperature of 30° C was chosen. Since the orientation of the fast axis of a Pancharatnam plate varies as a function of wavelength, the optimum solution for the entire polarimeter deviates somewhat from a simple pair of achromatic wave plates. Table 6 shows optimum values for the FeLCs. FeLCs with a retardation of 180° are constructed from two cells cemented together.

Calibration is done using a linear polarizer (Versalight) followed by a compound zero order quartz retarder. This retarder has a retardation of 0.25 waves at 400 nm or 0.16 waves at 587.6 nm. The calibration scheme uses sufficient combinations of orientations of the polarizer and retarder so that the retardation of the retarder is determined as part of the calibration.

Table 6. FeLC specifications determined from laboratory tests and modeling of polarimeter performance

FeLC ($\approx \circ$)	Material	Orientation (\circ)	Voltage (V)	Thickness (μm)	Type
180	9295	0.0	3.0	1.5	dual
180	9295	53.0	4.2	1.5	dual
180	9295	0.0	7.0	1.5	dual
102	8068	22.5	6.0	2.0	single
180	9295	93.4	3.0	1.5	dual
102	8068	22.5	7.0	2.0	single

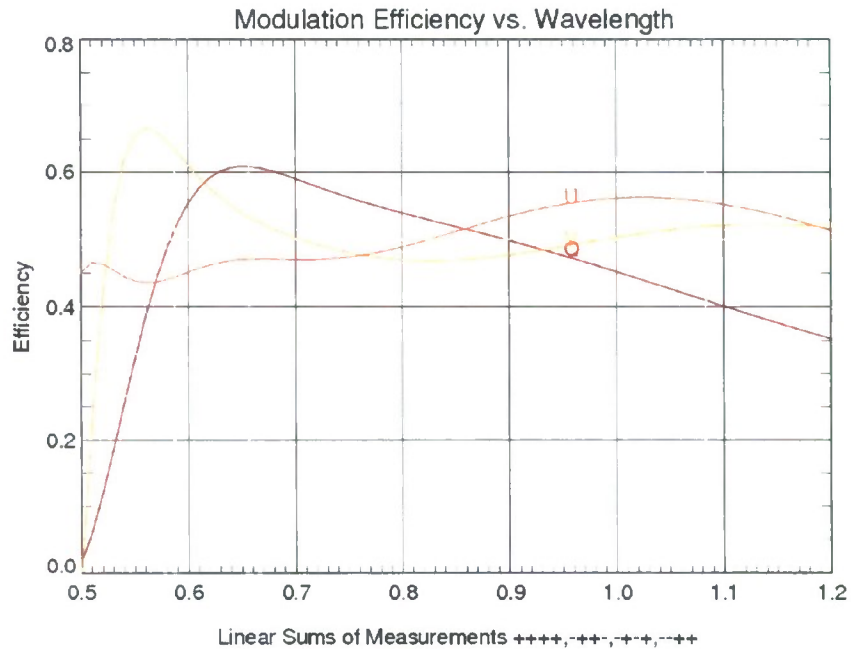


Figure 5. Modulation efficiency vs. wavelength. Shown are efficiencies for Q , U , and V . Note good efficiency near 0.5 or greater from 580 nm to 1100 nm

4. POLARIMETER CALIBRATION

ProMag is a dual-beam polarimeter, using an FeLC-based modulation stage and a dual-Wollaston beam-splitter. The modulator cycles through 4 different sets of voltages to achieve Stokes measurements. If we indicate with \mathbf{C} the 4-vector of the camera signals for one of the two beams, we can describe the polarimeter as a linear system characterized by a 4×4 transfer matrix \mathbf{T} , so that the system output (after a complete modulation cycle of the polarimeter) is given by

$$\mathbf{C}(\mathbf{T}; \mathbf{S}) = \mathbf{T} \cdot \mathbf{S}, \quad (1)$$

where \mathbf{S} is the Stokes vector of the radiation at the prime focus of the coronagraph. The main purpose of the calibration procedure is to determine the 16 elements of \mathbf{T} , for each of the two beams, so that once the polarimeter matrix is known, one can invert for the input Stokes vector from the camera output.

In calibration mode, the polarimeter is preceded by a linear polarizer, $\mathbf{P}(t, p, \alpha)$, of transmission t , partial polarization p , and position angle α , and by a retarder, $\mathbf{R}(t', r, \beta)$, of transmission t' , retardance r , and position

angle β . In the following we assume that the linear polarizer is ideal ($p = 1$), and not affected by positioning errors ($\Delta\alpha = 0$).

In calibration mode, the composite system of the polarimeter and the calibration optics is illuminated by radiation of unknown intensity and polarization. In the case of ProMag, since the polarimeter is placed at the prime focus of a refractive system, one can typically assume that the input radiation is completely unpolarized (in calibration mode, the sunlight is filtered by a diffuser placed in front of the telescope objective lens). More generally, this is only an approximation, and we must take into account the possibility that the input radiation may have some residual polarization, which also needs to be estimated.

In the presence of the calibration optics, Eq. (1) becomes

$$\mathbf{C}(\alpha, r, \beta, \tau; \mathbf{T}; \mathbf{S}) = \tau \mathbf{T} \cdot \mathbf{R}(r, \beta) \cdot \mathbf{P}(\alpha) \cdot \mathbf{S}, \quad (2)$$

with $\tau \equiv tt'$. For a quasi-ideal system, the true output is affected by (small) systematic errors over the set of parameters $\mathbf{Q} \equiv (r, \beta, \tau)$, associated with the calibration optics, which also need to be computed. Therefore we write the system output to first order as

$$\mathbf{C}(\alpha, r + \delta r, \beta + \delta\beta, \tau + \delta\tau; \mathbf{T}; \mathbf{S}) \approx \mathbf{C}(\alpha, r, \beta, \tau; \mathbf{T}; \mathbf{S}) + \delta\mathbf{Q} \cdot \frac{\partial}{\partial\mathbf{Q}} \mathbf{C}(\alpha, r, \beta, \tau; \mathbf{T}; \mathbf{S}), \quad (3)$$

having defined the error vector $\delta\mathbf{Q} \equiv (\delta r, \delta\beta, \delta\tau)$.

One problem we face right away is that, while we have an initial guess for the parameters of the calibration retarder, the overall transmission of the calibration optics, τ , the polarimeter matrix, \mathbf{T} , and the input Stokes vector, \mathbf{S} , are not known.

A first guess for the polarimeter matrix could be derived from the conceptual design of the polarimeter. In our case, a better option is to use a set of four independent calibration observations, assuming that the input radiation is completely unpolarized, and that the parameters of the calibration retarder are error free. In this case, from Eq. (2) we have

$$\bar{\mathbf{C}}_i = \mathbf{C}(\alpha_i, r, \beta_i, \tau; \mathbf{T}; I\mathbf{1}) = I\tau \mathbf{T} \cdot \mathbf{R}(r, \beta_i) \cdot \mathbf{P}(\alpha_i) \cdot \mathbf{1}, \quad (i = 1, 2, 3, 4) \quad (4)$$

where we put $\mathbf{1} \equiv (1, 0, 0, 0)^T$, and indicated with I the intensity of the input radiation at the prime focus.

A first guess for the total transmission of the calibration optics, τ , can be estimated by comparing the camera signals of observations taken with and without calibration optics. In fact, a "clear" observation of unpolarized radiation through an ideal polarimeter has elements (cf. Eq. [1])

$$(\bar{\mathbf{C}}_0)_i = I T_{i1}, \quad (5)$$

so we can derive an estimate of τ by comparing Eq. (4) and (5), for some appropriate set of calibration parameters, α and β . In fact, it is possible to show that $C_i(0, r, \beta, \tau; \mathbf{T}; I\mathbf{1}) + C_i(\pi/2, r, \beta, \tau; \mathbf{T}; I\mathbf{1}) = I\tau T_{i1}$, for any state (r, β) of the calibration retarder.

After this step, Eq. (4) can finally be used to determine a first guess of the polarimeter matrix, \mathbf{T}_0 , while from Eq. (1), applied to the "clear" observation of Eq. (5), we can estimate the input Stokes vector,

$$\mathbf{S}_0 = \mathbf{T}_0^{-1} \cdot \bar{\mathbf{C}}_0. \quad (6)$$

It must be noted that, for a typical polarimeter, *all* the elements of the first column of \mathbf{T} are the same, being equal to the overall transmission of the polarimeter. Such elements can then be fixed to 1 (i.e., $T_{i1} = 1$), since the polarimeter transmission enters Eqs. (1) and (2) as an overall factor, which can be folded into the mapping between the input Stokes vector and the camera signals. Therefore only 12 elements of the polarimeter matrix remain to be determined by the calibration procedure.

With these positions, the linear approximation to the calibration problem, Eq. (3), finally becomes

$$\begin{aligned} \mathbf{C}(\alpha, r + \delta r, \beta + \delta \beta, \tau + \delta \tau; \mathbf{T}; \mathbf{S}) \approx & \mathbf{C}(\alpha, r, \beta, \tau; \mathbf{T}_0; \mathbf{S}_0) + \delta \mathbf{Q} \cdot \frac{\partial}{\partial \mathbf{Q}} \mathbf{C}(\alpha, r, \beta, \tau; \mathbf{T}_0; \mathbf{S}_0) \\ & + \delta \mathbf{T} \cdot \frac{\partial}{\partial \mathbf{T}} \mathbf{C}(\alpha, r, \beta, \tau; \mathbf{T}_0; \mathbf{S}_0) + \delta \mathbf{S} \cdot \frac{\partial}{\partial \mathbf{S}} \mathbf{C}(\alpha, r, \beta, \tau; \mathbf{T}_0; \mathbf{S}_0), \end{aligned} \quad (7)$$

giving rise to a Newton-type iteration scheme,

$$\begin{aligned} \bar{\mathbf{C}} - \mathbf{C}(\alpha, r_k, \beta_k, \tau_k; \mathbf{T}_k; \mathbf{S}_k) = & \delta \mathbf{Q}_{k+1} \cdot \frac{\partial}{\partial \mathbf{Q}} \mathbf{C}(\alpha, r_k, \beta_k, \tau_k; \mathbf{T}_k; \mathbf{S}_k) \\ & + \delta \mathbf{T}_{k+1} \cdot \frac{\partial}{\partial \mathbf{T}} \mathbf{C}(\alpha, r_k, \beta_k, \tau_k; \mathbf{T}_k; \mathbf{S}_k) + \delta \mathbf{S}_{k+1} \cdot \frac{\partial}{\partial \mathbf{S}} \mathbf{C}(\alpha, r_k, \beta_k, \tau_k; \mathbf{T}_k; \mathbf{S}_k). \end{aligned} \quad (8)$$

The solution of this system requires a set of at least four independent calibration observations, with angle pairs (α_i, β_i) , for $i = 1, 2, 3, 4$, plus a “clear” observation, in order to invert for the 19 unknowns $(\delta \mathbf{Q}, \delta \mathbf{T}, \delta \mathbf{S})$. In order to avoid singularities in the linear system of Eq. (8), one should select a set of calibration configurations different from the one used in the solution of Eq. (4).

5. CONCLUSION AND FUTURE PROSPECTS

The Prominence Magnetometer is optimized for measurement of magnetic fields in prominences and filaments. It uses a low scattered light and polarization free telescope and a newly designed polarimeter optimized for the wavelength range 587.6 nm to 1083.0 nm. Routine operation starts the fall of 2008 with at least one two week long observing run scheduled each calendar quarter. This will allow for prominence magnetic field measurements of many targets during the ascending phase of the next solar cycle.

ACKNOWLEDGMENTS

We thank the NSO staff members, Scott Gregory, Ron Long, John Cornett, Wayne Jones, Tony Spence, and Steve Hegwer, who have helped with definition and fabrication of the new ESF prime focus assembly and for assistance in deploying ProMag.

REFERENCES

- [1] Leroy, J. L. *Astron. Astrophys.* **60**, 79 (1977).
- [2] House, L. L. and Smartt, R. N. *Solar Phys.* **80**, 53 (1982).
- [3] Landi Degl’Innocenti, E. and Landolfi, M., [*Polarization in Spectral Lines*], Kluwer Academic, Dordrecht (2004).
- [4] Landi Degl’Innocenti, E. *Solar Phys.* **79**, 291 (1982).
- [5] Querfeld, C. W., Smartt, R. N., Bommier, V., Landi Degl’Innocenti, E., and House, L. L. *Solar Phys.* **96**, 277 (1985).
- [6] Bommier, V., Landi Degl’Innocenti, E., Leroy, J. L., and Sahal-Br  chot, S. *Solar Phys.* **154**, 231 (1994).
- [7] Paletou, F., L  pez Ariste, A., Bommier, V., and Semel, M. *Astron. Astrophys.* **375**, L39 (2001).
- [8] L  pez Ariste, A. and Casini, R. *Astrophys. J.* **575**, 529 (2002).
- [9] Casini, R., L  pez Ariste, A., Tomczyk, S., and Lites, B. W. *Astrophys. J.* **598**, 67L (2003).
- [10] Casini, R., Bevilacqua, R., and L  pez Ariste, A. *Astrophys. J.* **622**, 1265 (2005).
- [11] Casini, R. and Manso Sainz, R. *J.Phys.B: At.Mol.Opt.Phys.* **39**, 3241 (2006).
- [12] Lites, B. W. *Appl. Opt.* **26**, 3838 (1987).
- [13] Socas-Navarro, H., Elmore, D., Pietarila, A., Darnell, A., Lites, B. W., Tomczyk, S., and Hegwer, S. *Solar Phys.* **235**, 55 (2006).
- [14] Gandorfer, A. M. *Optical Engineering* **38 Issue 8**, 1402 (1999).
- [15] Pancharatnam, S. *The Proceedings of the Indian Academy of Sciences* **41** (1955).